ECCOMAS Congress 2016
VII European Congress on Computational Methods in Applied Sciences and Engineering
M. Papadrakakis, V. Papadopoulos, G. Stefanou, V. Plevris (eds.)
Crete Island, Greece, 5–10 June 2016

ON THE APPLICATION OF MODERN TURBULENCE MODELS IN THE FLOW LAMINARIZATION PROBLEMS

Sergey L. Chernyshev[1], Alexander I. Ivanov[1], Andrey Ph. Kiselev[1], Dmitry S. Sboev[1], Leonid L. Teperin[1], Petr P. Vorotnikov[1], Valery V. Vozhdaev[1]

[1]Central Aerohydrodynamic Institute n.a. prof. N.E. Zhukovsky (TsAGI),
1, Zhukovsky st., 140180, Zhukovsky, Moscow reg., Russia
a-ph-kiselev@ya.ru

Keywords: Boundary Layer, Laminar-turbulent Transition, Turbulence Models, Experimental Investigation, Free-stream Turbulence, Boundary-layer Suction.

Abstract. *Analyzed are the results of experimental and computational studies of influence of the incoming flow turbulence level and boundary layer suction on the laminar-turbulent transition characteristics on straight and swept wings. The experimental investigations were carried out in the low-turbulence TsAGI T-124 wind tunnel. CFD-calculations were made basing on the numerical solution of the Reynolds-averaged Navier–Stokes equations (RANS). Turbulence models allowing predict the laminar-turbulent transition were used for closing the system of equations. The comparison is made of the predicted laminar-turbulent transition characteristics obtained using different turbulence models and the test data. The results of application of the semi-empirical e^N-method and simple empirical criteria for the transition prediction are also analyzed.*

1 INTRODUCTION

Numerical methods, based on the solutions of the Reynolds-averaged Navier–Stokes equations (RANS), are widely used nowadays. These equations are closed using semi-empirical turbulence models, with some models enabling in principle to calculate the laminar-turbulent transition.

The problems concerning the influence of the free stream turbulence and the extrapolation of the experimental data obtained in wind tunnels become very urgent in the process of the laminar airplane development. Various active methods of laminar-turbulent transition delay can be used, such as boundary layer suction, surface cooling or local heating, etc. Therefore it is necessary to have the numerical methods permitting calculate laminar-turbulent transition with acceptable accuracy both for wind tunnel and flight conditions, at different boundary conditions on streamlined surface. The validation of the transition prediction methods by comparison of experimental and calculated data obtained under the simulated influence of the above-mentioned factors is of great importance.

For this purpose the detailed experimental investigations of the transition zone on the straight and swept wings were carried out in the low-turbulence T-124 TsAGI wind tunnel. The influences of the incoming flow turbulence and acoustic disturbances were studied on the straight and swept wings models with laminar profile LV6 [1-3]. To increase the level of the flow turbulence, the turbulence grids were used. The effect of local boundary layer suction on the laminar-turbulent transition was studied on the model of low-sweep wing with the symmetric profile SR-0012 [4]. The air suction was realized through the slots in the model surface. The laminar-turbulent transition was detected using three independent methods: the china clay coating, the Stanton probes and the single-wire constant-temperature anemometer. The time-averaged and pulsating flow components in the boundary layer were measured by the hot-wire method.

The possibilities of application of different methods for prediction of the laminar-turbulent transition and for investigation of the increased free stream disturbances effect on the transition characteristics on the straight and swept wings models with laminar profile LV6 were analyzed earlier in conference papers [5, 6]. In particular, the measured characteristics of the boundary layer on straight wing were compared with the results of calculations based on the turbulence models of Langtry–Menter [7] and Walters–Cokljat [8]. The results of using the semiempirical e^N-method and some simple empiric criteria for prediction of laminar-turbulent transition both for straight and swept wings with LV6 profile also were analyzed.

In the present paper the application is studied of modern turbulence model [9] based on the transport equation for the intermittency, to prediction of the laminar-turbulent transition on the swept wings surfaces for both the increased turbulence level of the incoming flow and the presence of the boundary layer suction. Comparison is made of the predicted laminar-turbulent transition characteristics for straight and swept wings with the LV6 airfoil. The comparative analysis of the computed boundary layer parameters and the experimental data is fulfilled [1-4].

2 AERODYNAMIC FACILITY

The experimental investigations of the effects of the incoming flow turbulence and local boundary layer suction on the laminar-turbulent transition on straight and swept wings were carried out in the low-turbulence T-124 TsAGI wind tunnel [10].

TsAGI T-124 subsonic wind tunnel (velocity range – $U_0 = 2\ldots100$ m/s) is a closed-circuit compressor wind tunnel with test section dimensions of 1 m×1 m×4 m. Wind tunnel T-124 is remarkable for sufficiently low initial turbulence level and low noise. These characteristics

were achieved by means of applying high contraction ratio in the nozzle (17.6), high accuracy of maintaining the fan speed, using deturbulizing meshes in the settling chamber with the inner cell size of 0.7 mm, applying diffuser with a small opening angle, thorough finishing of the inner surfaces of the facility's channels and making of wood almost all basic elements of the wind tunnel with the exception of the test and fan sections. So, for the flow speed of less than 80 m/s the level of initial turbulence appears to be only 0.05%. It creates favorable conditions for researches of the boundary layers development leading, in the end, to the laminar-turbulent transition.

3 INVESTIGATIONS OF THE INFLUENCE OF INITIAL FLOW TURBULENCE LEVEL ON THE LAMINAR-TURBULENT TRANSITION ON STRAIGHT AND SWEPT WINGS WITH LAMINAR PROFILE LV6

3.1 Description of the models and experimental techniques

The tests described in this section are the continuation of the researches completed in TsAGI in the framework of the TELFONA project (6^{th} European FP) [1], which are devoted to investigations of the possibilities of implementation of different calculation methods to the predictions of the laminar-turbulent transition and the influence of higher disturbance background level on its characteristics.

The LV6 airfoil model is a rectangular wing with the chord of 1000 mm and the span of 998 mm. This airfoil was designed by DLR as part of the TELFONA Pathfinder Wing design activity. The shape of the laminarized airfoil is close to symmetric one. The model is placed in the closed test section of the wind tunnel T-124 from wall to wall at the equal distances from the floor and from the ceiling. Since such wing position permits to avoid the formation of tip vortices, the modeling of the flow over the "infinite span" wing is performed in the best way and the flow in the middle section of the model may be considered as two-dimensional. The photographs of the 2D LV6 airfoil model before and after installation in the test section of the T-124 wind tunnel are shown at Figure 1. The right photo shows also the *XZ*-traverse sting, the sting extender and *Y*-traverse gear.

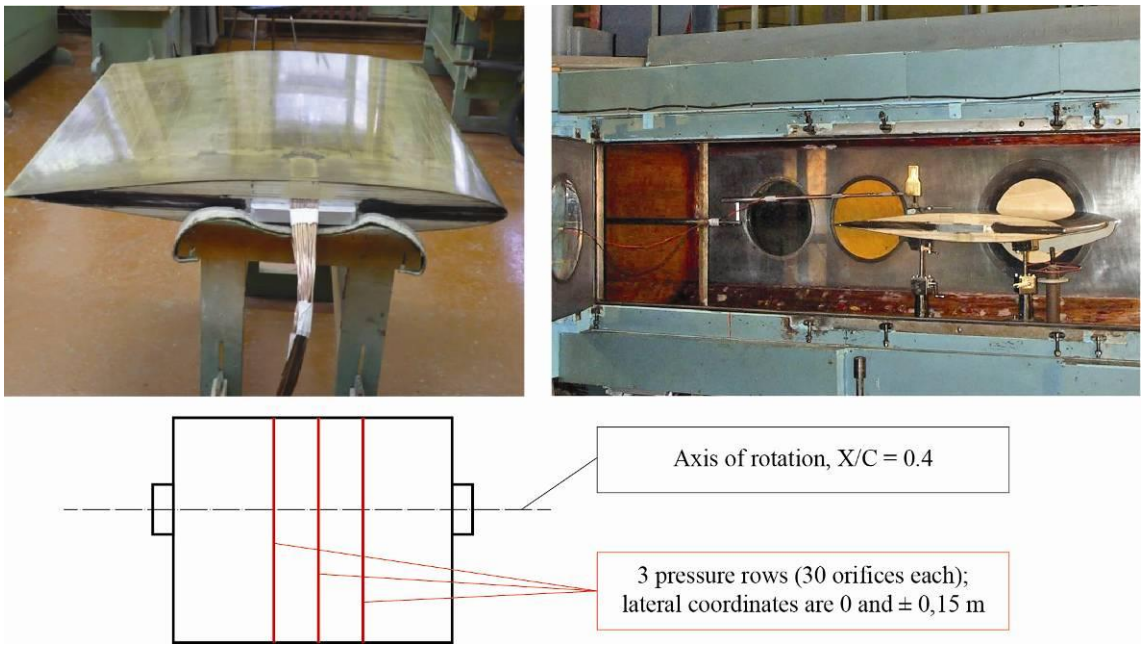

Figure 1: 2D LV6 airfoil model before and after installation in the test section of the T-124 tunnel

The second model has been tested is the wing section model with the sweep angle $\chi = 35°$, with the chord length along the free stream direction $C = 1000$ mm and the span of 998 mm. This model has the same shape of the LV6 laminar airfoil in the section along free stream direction, with the relative thickness of 11%.

In the closed test section of the T-124 wind tunnel the swept wing model was also placed at the equal distances from the floor and from the ceiling from wall to wall. The overview of 2.5D swept wing model with 3D traverse gear in T-124 wind tunnel test section is presented in Figure 2. In order to prevent the spreading additional disturbances along leading edge from the junction area of the wing and right side (in stream direction) test section wall, the model was equipped with the fence. The fence was fixed at distance of 120 mm from the right wall of the test section.

Figure 2: 2D LV6 airfoil model before and after installation in the test section of the T-124 tunnel

Regimes at angles of attack $\alpha = -2°$ and 0 were chosen for further investigations in swept wing boundary layer. Both models have the relative thickness of 11%. The experiments were conducted at free stream velocity $U_0 = 80$ m/s that correspond to Reynolds number 5.5×10^6 based on full chord of the model and Mach number 0.24. The system of coordinates was used with the longitudinal axis X directed perpendicularly to the leading edge of the wing, and the transversal axis Z directed along the leading edge.

The objective of the test was to study the transition mechanism associated with the Tollmien-Schlichting waves or cross-flow instability development in the 2D flow or infinite swept wing condition. Before the main tests, it was necessary to make certain that in the central part of the models there are areas in which the flow parameters do not depend on the lateral coordinate Z. For this purpose both models were equipped with three rows of pressure taps (Figure 1). Also before the main measurements the Y-traverse influence on the averaged flow was investigated by means of the model pressure distributions comparison for two test conditions – with and without the Y-traverse gear. Data analyses showed that the traverse gear influence on the pressure distributions was rather small [1, 2].

For both 2D and 3D cases at $\alpha = 0$ the pressure distributions have the following specific features: after the domain of flow acceleration ($X/C < 0.15$) there is a region practically without the pressure gradient. In this zero pressure gradient region the measured boundary layer velocity profiles coincide very well with Blasius solution for 2D case. On swept wing model there is favorable pressure gradient region at $\alpha = -2°$, $0 < X/C < 0.5$.

The hardware component of the measuring system used consists of the single hot-wire with CTA DISA 55D01, a container for 32 pressure transducers, and an automatized traverse gear, which are connected to the PC through the input/output subsystem.

The experiments were carried out at three flow regimes: at the natural conditions of the wing tunnel test section and with the elevated free-stream turbulence level generated by two grids. Grids were installed at the point of entry to the test section. Turbulence level Tu_u (based on longitudinal component of pulsations u_{rms}) at the model leading edge estimated by the values of 0.7% for grid № 1 and 1.1% for grid № 2. Turbulence level Tu (based on three components of pulsations) at the model leading edge estimated by the values of 0.61% for grid № 1 and 0.91% for grid № 2 due to some degree of anisotropy of generated turbulence (v_{rms}/u_{rms} = 0.73…0.78). For natural conditions Tu = 0.064%. The Taylor micro-scale of turbulence for the longitudinal pulsations appeared to be equal to 5–6 mm for both grids. Longitudinal integral turbulence scale was made by means of integration of the autocorrelation function. For grid № 1 the value of this scale was 21.3 mm and 44.7 mm for grid № 2.

In all experiments the region of laminar flow destruction was determined by studying the intermittency γ in the boundary layer. The following model [11] for γ was used in the transition region

$$\gamma = 1 - \exp\left[-\frac{n\sigma}{U_0}(X - X_t)^2 \right],$$

where X_t is the coordinate of the transition inception, n is the rate of turbulent spots generation in the domain of their emergence, and σ is a kinematic parameter depending on the velocity and angle of propagation of turbulent spots. It was demonstrated [11, 12] that this dependence can be used to describe transition regions in various flows. In particular, in the majority of flows, the function

$$F = \sqrt{-\ln(1-\gamma)}$$

in the transition region could be approximated by a straight lines. The crossings of these lines with X axis were chosen as X_t positions, while the value γ = 0.99 (F = 2.14) was chosen to specify the location of transition completion X_T. In order to characterize transition location with single parameter the position where γ = 0.5 is referred below as $X_{0.5}$. $\Delta X = X_T - X_t$ gives the length of transition region.

All intermittency measurements were performed at the height in the boundary layer corresponding to U/U_e = 0.5, i.e. in the middle of boundary layer (U_e is local external velocity). It allowed conducting the measurements in 3D boundary layer with single-wire probe, because the angles between direction of U_0 and local streamline at this height in the measurements region didn't exceed 2–4° so resulting error didn't exceed 2%. The additional details of experimental techniques could be found in [2, 3].

3.2 Modelling of laminar-turbulent transition on the basis of numerical solutions of the Reynolds-averaged Navier–Stokes equations

Calculations were performed on the basis of numerical solutions of the Reynolds-averaged Navier–Stokes equations, implemented in the software package ANSYS CFX (TsAGI's License №501024).

The mathematical model of the test section, as well as the geometry and the positions of the wings in the wind tunnel fully comply with the conditions of the experiment.

Turbulence models are used to close the Navier -Stokes equations which enable in principle to calculate the laminar-turbulent transition [7-9] .

Model $\gamma - \mathrm{Re}_\theta$ [7] was developed by F. Menter and R. Langtry on the basis of the shear stress transport (SST) equation model. The transition characteristics are defined using the intermittency coefficient γ and number $\tilde{\mathrm{Re}}_{\theta_t} = \rho\theta U / \mu$, corresponding to Reynolds number at the transition beginning, defined using the local velocity U and momentum thickness θ. Both parameters, γ and $\tilde{\mathrm{Re}}_{\theta_t}$ are defined from the solution of the corresponding differential transport equations.

The results of the CFD-studies of the laminar-turbulent transition on the straight wing completed using $\gamma - \mathrm{Re}_\theta$ Langtry and Menter model and another well-known model of the laminar-turbulent transition by Walters and Cokljat [8], are presented in paper [5]. Compared with the Walters and Cokljat transition model based on the transport equations for laminar and turbulent kinetic energy, Langtry and Menter model demonstrates more reliable results.

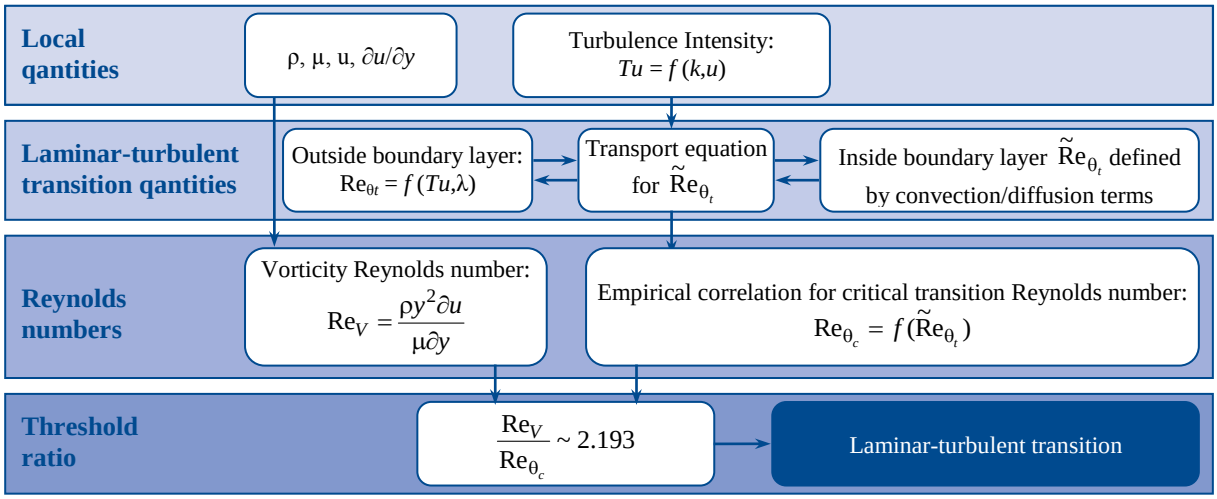

Figure 3: The block - scheme of calculating the position of laminar - turbulent transition on the basis of the model Langtry–Menter [7]

For calculations by means of the ANSYS CFX software the unstructured finite-difference mesh was generated. The total number of nodes in the computational domain reached 11 million and the nodes were combined into volume elements (tetrahedra and prisms). The total number of volume elements is 26.5 million, the total number of tetrahedra being 6.8 million. An additional thickening of mesh was made on the upper surface of the wing, as a result of which the maximum size of an element on the upper surface did not exceed 3 mm.

The turbulence intensity is defined experimentally, as a rule, in the aerodynamic model installation zone. In the numerical methods the turbulence intensity is specified at the inlet to the computational domain. There may be some turbulence attenuation depending on the distance from the inlet to the computational domain x^* to the model.

In modern computational models the turbulence intensity decay is calculated as follows:

$$Tu = Tu_0 \left\{ 1 + \frac{3\rho U \beta Tu_0^2}{2\mu R_T} \cdot x^* \right\}^{-\left(0.5\frac{\beta^*}{\beta}\right)}. \qquad (1)$$

Here U – mean convective velocity, Tu_0 – initial turbulence intensity; ρ – density, β and β^* – constants of the SST (Shear Stress Transport) model of turbulence.

Relative turbulent viscosity R_T is defined as:

$$R_T = \frac{\rho k}{\mu \omega},$$

were ω – the specific rate of dissipation of turbulent energy; k – turbulent kinetic energy.

In the experiments of [1-3] the turbulence intensity was measured in the vicinity of the wing leading edge and it was 0.0637% under natural conditions. On the basis of formula (1) it is possible to obtain the required turbulence intensity at a given distance from the inlet to the computational domain (Figure 4).

It should be noted that in calculation of the wing flow characteristics, the relative turbulent viscosity was taken equal to 1. The values of constants in the SST turbulence model β and β^* were taken 0.09 and 0.0828, respectively. As a model of laminar-turbulent transition the $\gamma - \mathrm{Re}_\theta$ – model of Langtry and Menter was used. The following computational results were obtained using standard values of the model constants.

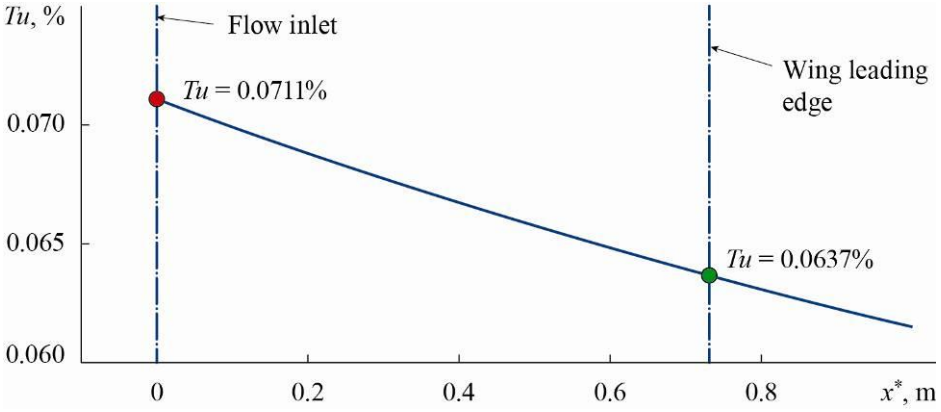

Figure 4: Decay of turbulence intensity depending on the distance downstream

Reynolds-averaged Navier–Stokes equations are closed using the semi-empirical turbulence models. However only few of turbulence models allow predict the laminar-turbulent transition (Figure 5).

Transition on the swept wing is essentially triggered by the instability of the cross-flow, and the presence of both positive and negative pressure gradients contributes to the instability. In the turbulence models of Langtry and Menter [7] and Walters and Cokljat [8] the cross-flow instability is not taken into account.

Further development of $\gamma - \mathrm{Re}_\theta$ turbulence model became new Local-Correlation-Based Transition Modelling (γ-model) model developed by Menter and Smirnov [9], in which the possibility of taking into account the crossflow instability was realized.

It only solves one equation for the intermittency γ and is again based strictly on local variables. Significant effort was invested in ensuring a simple formulation with a limited number of user accessible constants, which allow the fine-tuning of the model for specific applications. Finally, an additional indicator was developed, which allows the detection of crossflow instabilities and allows its connection to the Arnal C1-criterion [13].

It should be noted that since γ-model of turbulence [9] does not involve the transport equation for the transitional Reynolds number, this gives a reduction in calculation time compared with the time of the calculations based on the $\gamma - \mathrm{Re}_\theta$ model of Langtry and Menter applied to calculate the laminar-turbulent transition characteristics on a straight wing.

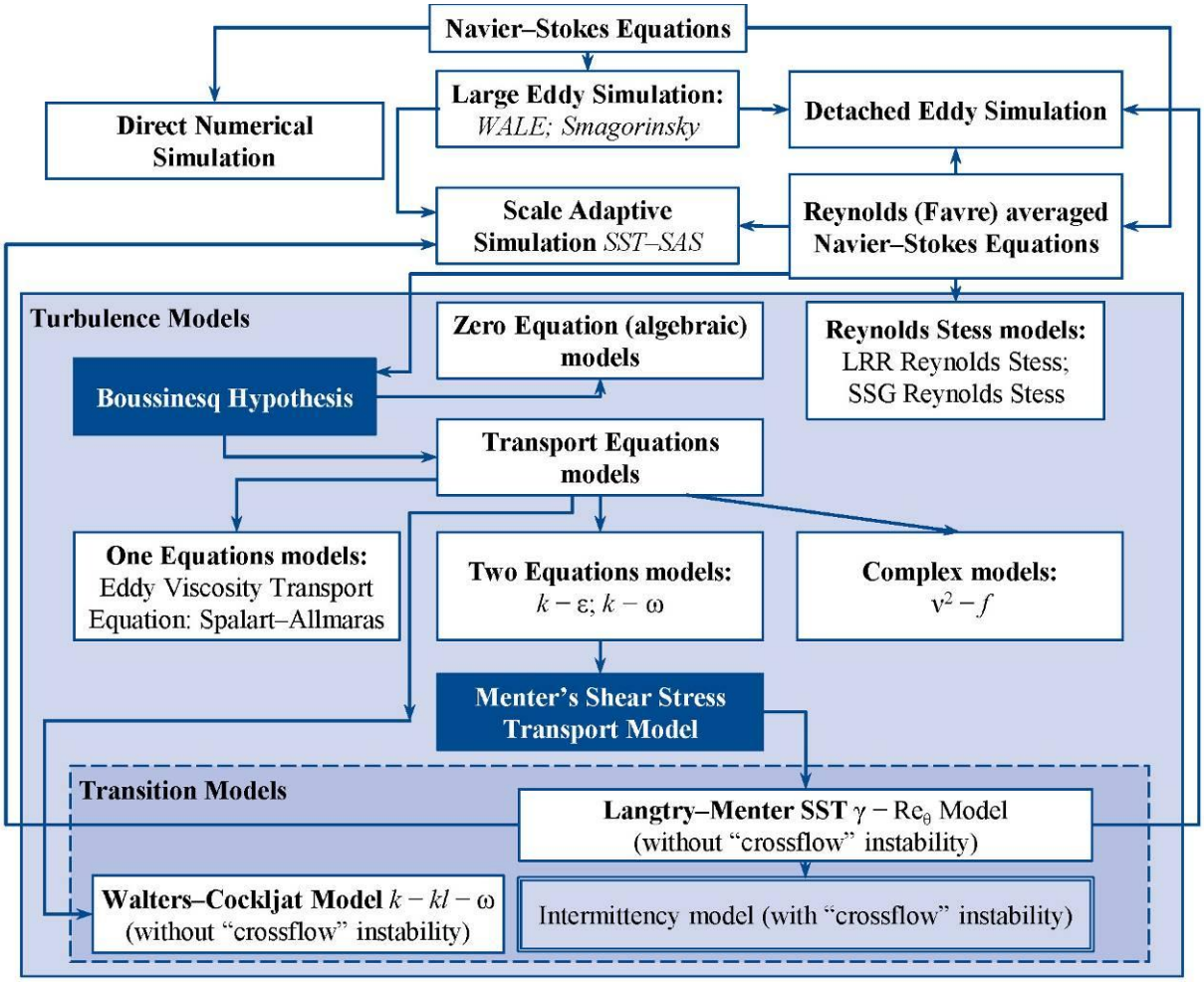

Figure 5: Classification advanced turbulence models

Comparison of experimental and calculated pressure distribution in the central section of the upper surface of the wing at zero angle of attack is shown in Figure 6. The dashed-dotted line shows the conversion of the pressure distribution on the straight wing to the oblique wing with the same flow chord according to the infinite swept wing rule of the linear theory.

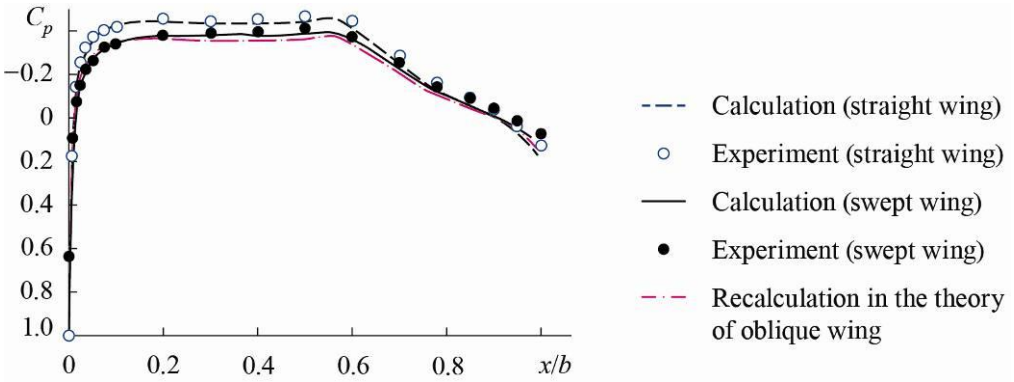

Figure 6: The pressure distributions on the upper surface of wings at $\alpha = 0$

Experimental and calculated intermittency distributions at natural disturbances background in the central section of swept and straight wings, indicating the beginning of the laminar-turbulent transition in the boundary layer, the length of the transitional area and the beginning of fully tur-

bulent flow, are shown in Figure 7. It should be noted that the use of γ-model in the calculation of the laminar-turbulent transition on swept wings for this type of flow provides fairly good accuracy.

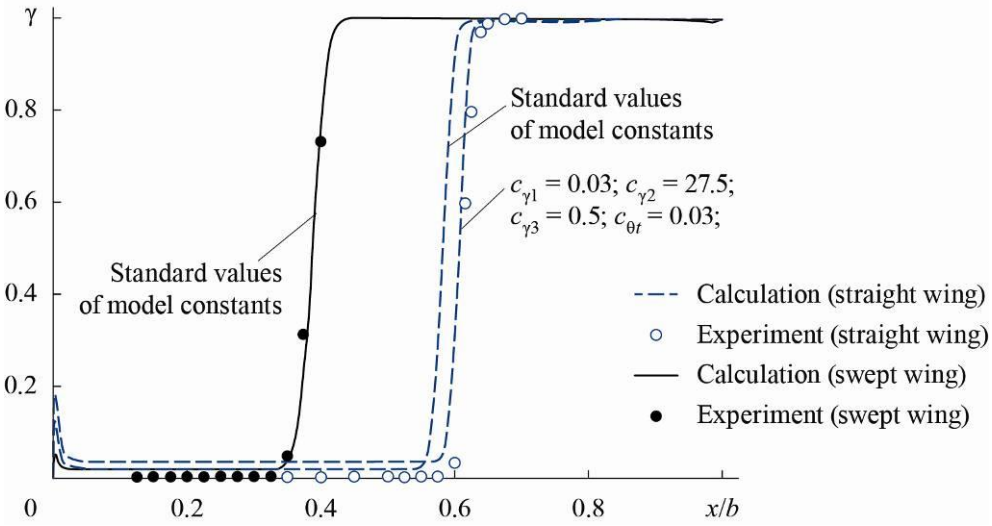

Figure 7: Distribution of intermittency γ on the upper surface of the wings at α = 0 and *Tu* = 0.064%

On the straight wing with the standard values of the model constants of the $\gamma - \mathrm{Re}_\theta$ model there are some differences between the calculated and experimental data (Figure 7). However, conducted computational studies on the effect of constants of the $\gamma - \mathrm{Re}_\theta$ model used to calculate the laminar-turbulent transition on a straight wing, allowed set the values of model constants that provide a good agreement between the calculated and experimental data

In experimental studies [1-3] on the effect of free-stream disturbances on the boundary layer transition the initial turbulence was varied by installation turbulizing grids at the entrance to the test section of WT. According to the measurements of pulsations in the WT without models at a distance of 2.4 m from the grid, it was found that in the vicinity of the model leading edge the turbulence increases to 0.61% in case of installation of the grid No. 1, and increases to 0.91% in case of installation of the grid No. 2.

As already mentioned above, the degree of turbulence defined at the inlet to the computational domain attenuated too fast compared with the experimental data. In this regard, the inlet to the computational domain was placed closer to the wing model. The turbulence intensity in the boundary condition at the flow inlet to the computational domain was set according to the formula (1) so that in the wing area the degree of turbulence corresponded to the experimental data. In this regard, the inlet in the computational domain was moved closer to the model of the wing. The calculations used γ–model of turbulence with standard values of the constants.

Figure 8 shows the intermittency distribution near the surface of the wing in its middle section. This restructure of the computational domain significantly affected the results of the calculation at the natural background of flow disturbances (*Tu* = 0.064%). Comparison of the calculated and experimental results shows that in the absence of turbulizing grid γ-model predicts earlier laminar-turbulent transition compared with the experimental data.

With increased degree of turbulence corresponding to the turbulizing grid No. 1, the CFD prediction demonstrates sharper increase of intermittency in the laminar-turbulent transition zone, but what concerned the position of the point of the transition beginning, calculated and experimental data are in satisfactory agreement (Figure 8). The computational prediction of the character of the intermittency changes corresponding to the presence of grid No. 2 are in good agreement with the experimental data.

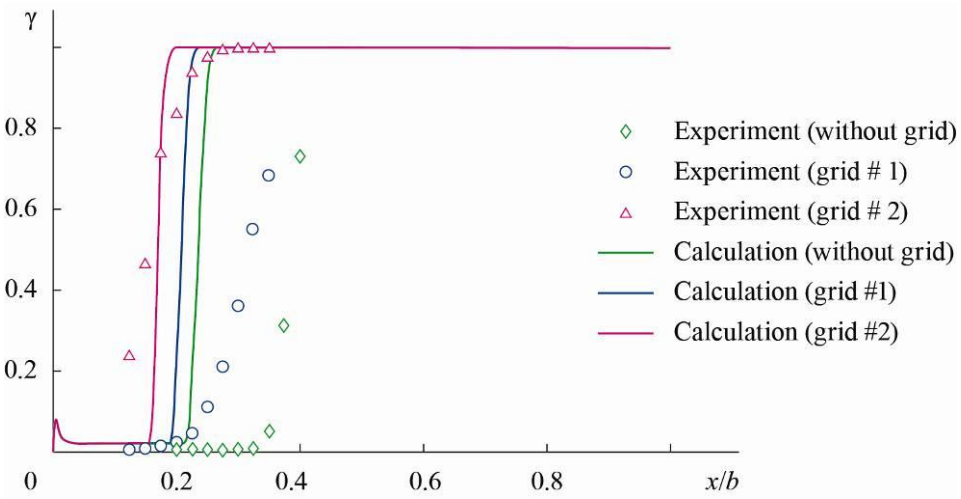

Figure 8: Distribution of intermittency in the central section on the upper surface of the swept wing at zero angle of attack

At the angle of incidence $\alpha = -2°$ without turbulizing grids calculation gives more upstream position of the laminar-turbulent transition compared with the experimental one (Figure 9). At the presence of both turbulizing grids the position of the laminar-turbulent transition shifts forward approximately at the same distance (Figure 9). The experiment shows similar effect. Visualization of the skin friction coefficient, demonstrating the calculated position of the laminar-turbulent transition, is shown in Figure 10.

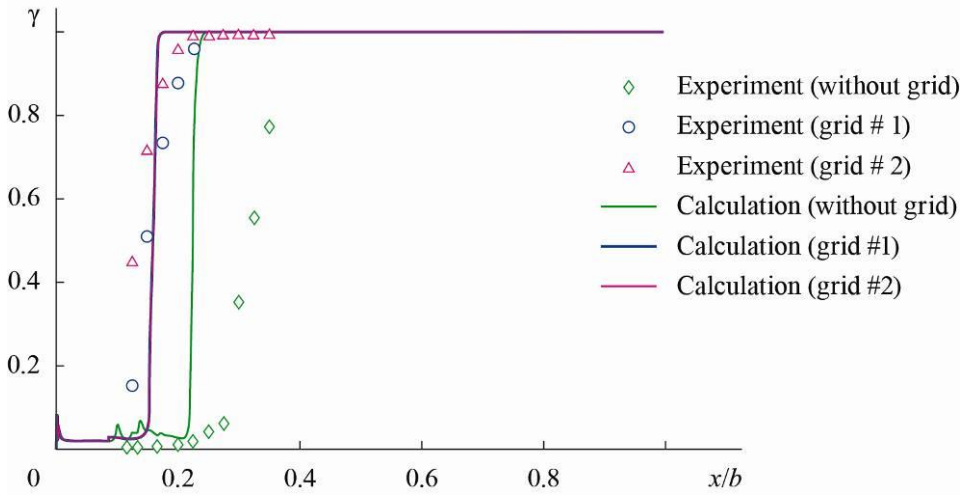

Figure 9: Distribution of intermittency in the central section on the upper surface of the swept wing at $\alpha = -2°$

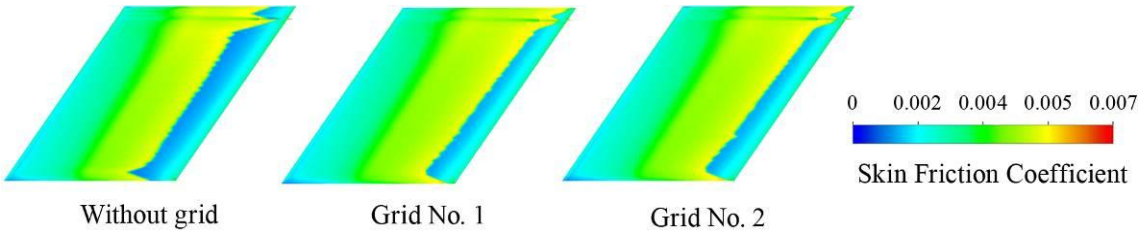

Figure 10: Distributions of skin friction coefficient on the upper surface of the swept wing at $\alpha = -2°$

3.3 The results of using of semiempirical e^N-method and some simple empiric criteria

Regardless of a significant progress in the development of numerical methods, empirical and semi-empirical models of the transition are still widely used in engineering practice.

The results of using of some simple empiric criteria and semiempirical e^N-method for prediction of laminar-turbulent transition both for straight and swept wings with LV6 profile were analyzed in the papers [5, 6] and [14].

For 2D boundary layer at the elevated free-stream-tyrbulence levels the transition length was calculated using models by Mayle [12], Solomon *et al.* [15] and Roberts & Yaras [16].

Also in 3D case for low turbulence environment three simple empirical transition criteria were applied, namely, Arnal C1 [13], Brown [17], and Barinov–Lutovinov [18]. Finally, semi-empirical model recently developed by Ustinov [19] for free-stream-induced transition was tried. It based on transient growth idea with subsequent secondary instability of streaks.

For calculation of hydrodynamic stability characteristics of 2D and 3D three-dimensional boundary layers on the LV6 straight end swept wings general numerical matrix method developed in TsAGI was used [20]. The computation of eigenvalues is performed for real counterpart of initial complex matrix with the use of QR-algorithm. For 2D flow the *N*-factors were computed using envelope method.

For definition of the laminar-turbulent transition location in the range $0.1\% \le Tu \le 1\%$ L.M. Mack [21] proposed the empirical dependence of *N*-factor vs. *Tu*.

The calculated values of the *N*-factor for 2D boundary layer are compared with the Mack's relation in Figure 11. In the case Grid No. 2, correlation overpredicts the *N*-factor of the transition. At $Tu = 0.61\%$, the criterion yields feasible results, especially if the value corresponding to the $X_{0.5}/C$ is treated as the transition point. In Grid No. 1 and Grid No. 2 cases, the *N*-factors corresponding to X_t/C are equal to zero, i.e., the transition started in these situations before the boundary layer lost its stability (by-pass transition). For natural conditions ($Tu = 0.064\%$) the laminar separation with turbulent reattachment were observed with the value of $N = 13.5$ at separation.

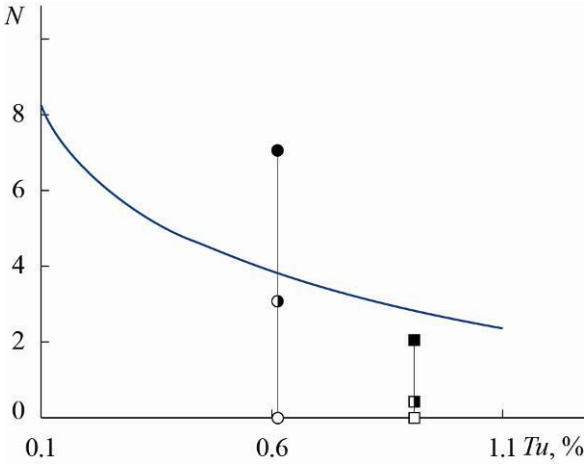

Figure 11: Dependence of the transition *N*-factor on the free-stream turbulence level for 2D flow. The solid line shows the Mack relation [21], open symbols corresponds to the X_t, solid symbols to the X_T, the half-open symbols refers to the $X_{0.5}$

Because in the 3D boundary layer the external turbulence influence can't be reliably taken into account nowadays using the e^N-method, for comparison the experimental data, which were obtained at the low-turbulence external flow should be used. In these conditions the transition line on the swept wings has the serrated form, with critical *N*-factor values for other

values of spanwize co-ordinate possibly being slightly different from the obtained ones. However, the dimension of turbulent wedges in the longitudinal direction usually do not exceed 10% of the chord, giving rise to the error in definition of the critical *N*-factor values no more than ±1.

The calculated longitudinal distributions of the *N*-factor for the cases of angles of attack of $\alpha = 0$ and $-2°$ are shown in Figure 12.

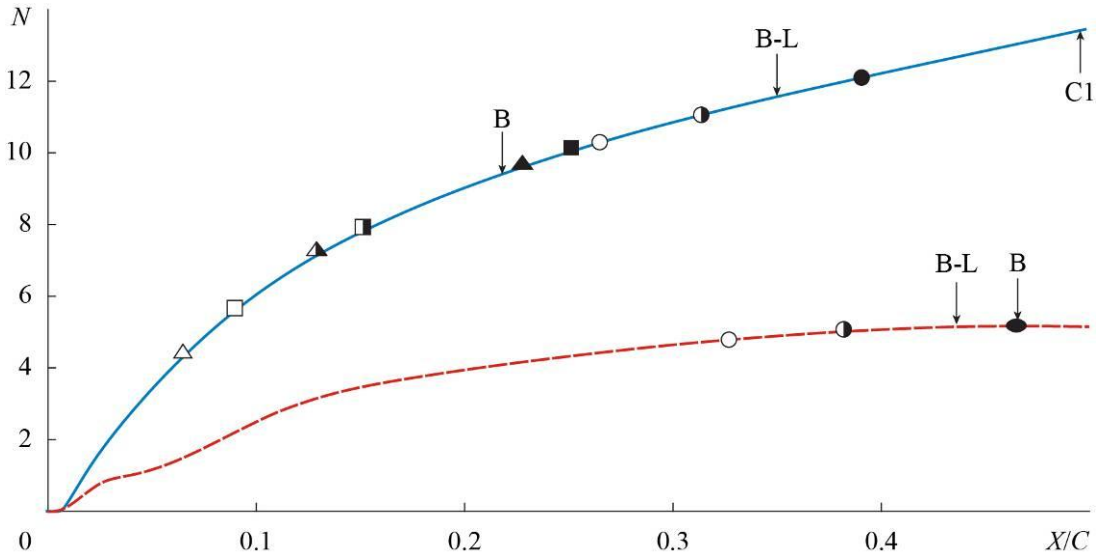

Figure 12: N-factor dependence from the longitudinal co-ordinate: solid line – $\alpha' = -2°$, dashed line – $\alpha' = 0$, ○ – natural condition, $Tu = 0.064\%$, □ – $Tu = 0.61\%$, △ – $Tu = 0.91\%$. Open symbols show the transition onset, filled symbols – points, where $\gamma = 0.99$, semi-filled – position $\gamma = 0.5$. Shooters showed the transition location defined by means of criteria C1, Brown (B) and Barinov-Lutovinov (B-L).

The specific points obtained at different experimental conditions are also marked on these curves. Figure 12 demonstrates that at zero angle of attack the calculated *N*-factor values are substantially lower than at $\alpha = -2°$. It is explained by the fact that according to calculations the cross-flow intensity at $\alpha = 0$ is approximately two times lower than at $\alpha = -2°$. At $X/C = 0.2$ typical values of the maximum cross-flow velocity in the co-ordinate system associated with the inviscid flow streamline are equal to $0.023U_0$ and $0.042U_0$ respectively for these two cases. *N*-factor value corresponding to $\gamma = 0.5$ for low-turbulence external flow in the case of $\alpha' = -2°$ was 11.1. This value practically coincides with the well-known data [22] for the tests in the low-turbulence wind tunnels in the presence of cross-flow instability. However, for the same external conditions at $\alpha = 0$ the *N*-factor value corresponding to $\gamma = 0.5$ appeared to be only 5. This value is substantially lower than *N*-factors, obtained in the condition of the increased turbulence at $\alpha = -2°$, where they were 7.9 for $Tu = 0.61\%$ and 7.1 for $Tu = 0.91\%$ (see Figure 12). It should be noted especially that in all calculation cases the cross-flow instability waves has become the most quickly rising ones. In both the experiment and calculations the evidence of the longitudinal instability (like the Tollmien-Schlichting waves) was unimportant. So, it may be concluded that contrary to the 2D flows, for the swept wing boundary layer the semi-empirical e^N-method (in the variant of the envelope method) gives substantial scatter of the critical *N*-factor values and does not permit to correlate reliably the transition data. In the papers [22, 23] similar conclusions were drawn also for other variants of e^N-method. The reason of this phenomenon is dominating of the non-linear effects in the transition processes in the 3D boundary layer even at low level of the external turbulence.

The results of implementation of the criteria [13, 17,18] for definition of the transition location in the conditions of the described experiments are also shown in Figure 12. It is shown, that C1 criterion [13] at $\alpha = -2°$ gives shifted downstream transition location, and at $\alpha = 0$ this criterion predicts absence of transition up to the separation line in the adverse pressure gradient zone. Brown criterion [17] has scatter of about 10% of the chord length relative to $\gamma = 0.5$ point in both positive and negative. The best results were demonstrated by the criterion of Barinov and Lutovinov [18], which in both cases predicts the transition location shifted downstream from the point $\gamma = 0.5$ by approximately 5% of the chord, i.e. corresponding to $\gamma \approx 0.8$.

The important findings of the analyses [5, 6] and [14] can be briefly summarized as following:

- The empirical and semi-empirical models, allowing estimate the transition location basing only on the averaged flow characteristics are still very robust and effective means for laminar-turbulent transition prediction at elevated free-stream turbulence level, at least in 2D boundary layers. Some of empirical criteria permit to evaluate the transition location on the swept wings, but they can't be applied at high free-stream turbulence level.
- The e^N-method rather successfully correlates with laminar-turbulent transition for 2D boundary layer; however, the values of *N*-factor corresponding to transition are substantially different for various external conditions. Contrary to the 2D flows, for the swept wing boundary layer the semi-empirical e^N -method gives substantial scatter of the critical *N*-factor values and does not permit to correlate reliably the transition data. The reason of this phenomenon is dominating of the non-linear effects in the transition processes in the 3D boundary layer even at low level of the external turbulence.
- In 3D boundary layers at some specific combinations of the pressure distribution and free-stream turbulence-level the very uncommon ways to transition could be existed. So, it was found that the transition location on the swept wing at high free-stream turbulence shifts downstream compared with the straight wing tests. This fact contrasts sharply with the available data concerning the sweep angle influence on the transition location at the low-turbulence external flow. This fact must be accounted for careful planning of experiments in industrial wind tunnels.

4 STUDIES OF SUCTION EFFECT ON THE LAMINAR-TURBULENT TRANSITION ON THE LOW-SWEPT WINGS WITH SR-0012 PROFILE

4.1 Experimental investigations

The experiments [4] were conducted on a wing at zero angle of attack and values of freestream speed from 30 to 90 m/s. For this speed range the free-stream turbulence level changes from 0.03 to a 0.07%.

The influence of suction on flow regime in the boundary layer was investigated on the upper surface of a wing with the following characteristics: symmetrical airfoil section, sweep angle $\chi = 15°$, thickness-to-chord ratio 12%, chord C= 800 mm, span L = 1 m (equal to the test section width). Three slots were made on the wing upper surface with length and width l_0 = 535 mm and $h \sim 0.15 \div 0.2$ mm, respectively. The Reynolds number of the slot is defined as $\mathrm{Re}_{i,s} = v_w h/\nu$, where v_w – average speed of flowing in a slot, ν – kinematic viscosity coefficient, and, the full air expense through a slot $Q_i = v_w h l_0$, i – number of slot.

The view of the model in the test section of T-124 WT is presented at Figure 13. The scheme of the suction slots location on the wing is shown at Figure 14.

Figure 13: The photo of model in test section of T-124 WT

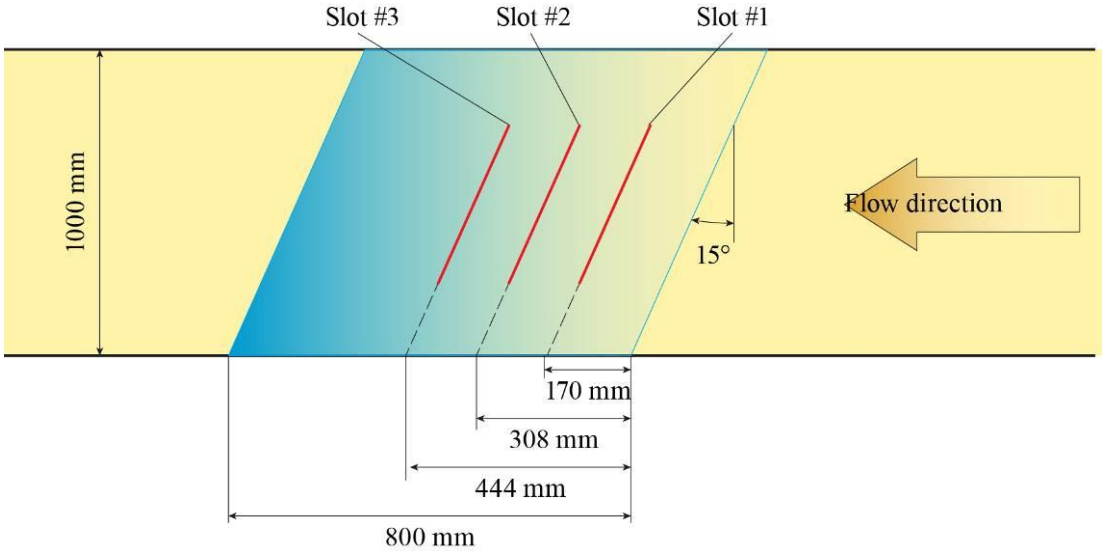

Figure 14: Scheme of the suction slots location on the wing

The wing surface was carefully polished. The wing's construction provided autonomous and spanwise uniform air suction through any of the slots.

Positioning of laminar-turbulent transition at the upper surface of the wing was performed at the same speed V_∞ = 40 m/s. Identification of flow regimes in the boundary layer on the model was carried out with the help of three independent methods: with kaolin coating on the lover surface (i.e., in the absence of suction), and on the opposite surface using a modified razor-blade technique and by measuring the variation of the intensity of the longitudinal velocity fluctuations ε near wall with a hot-wire anemometer and remotely-controlled traversing gear.

The razor-blade technique turned out to be effective in determining transition zone as well. The coordinates of the beginning of the transition zone, $\overline{X}_t = X_t/C$, obtained with hot-wire anemometer are presented in Figure 15.

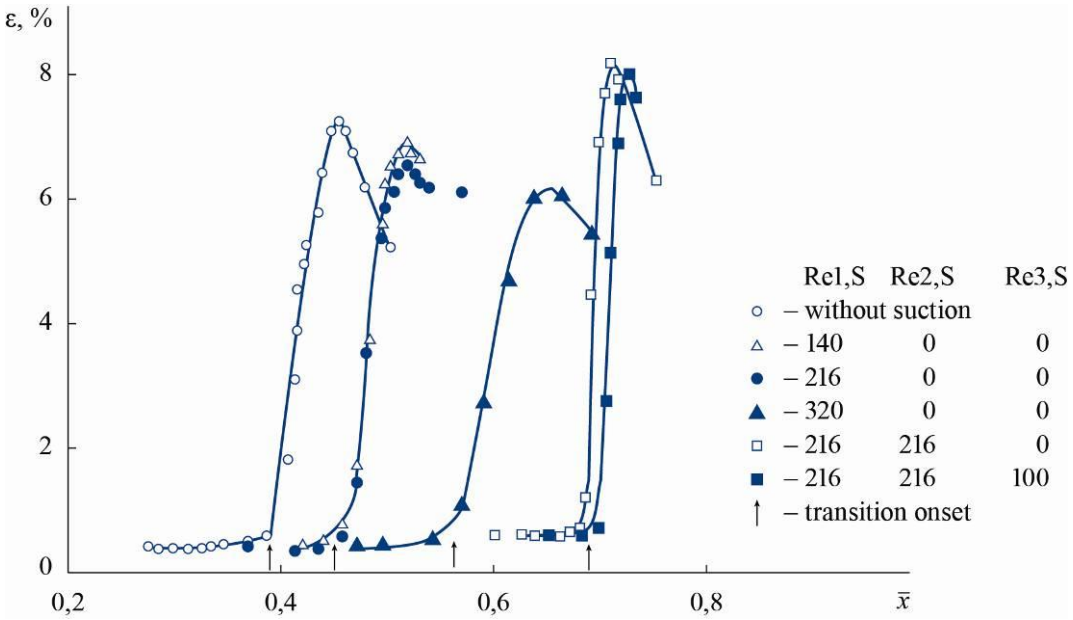

Figure 15: Measured variations of the intensity of the longitudinal velocity fluctuations ε near wall

According to this data, $\overline{X}_t = 0.392$ in the case when the suction is absent. The increase in the suction intensity through the first slot to $Re_{1,s}$ = 216, did not practically affect the transition onset position: the coordinate $\overline{X}_t$ turned out to be 0.45. But having increased $Re_{1,s}$ to 320, this point moved to $\overline{X}_t = 0.56$. The simultaneous suction from the first and second slots at $Re_{1,s} = Re_{2,s}$ = 216 resulted in displacing the transition onset position to $\overline{X}_t = 0.685$. The addition of suction through the third slot did not practically influence the transition onset position: in this case $\overline{X}_t$ was equal to 0.69. It should be born in mind that in the two latter cases transition was caused by the separation of the boundary layer which cannot be prevented with suction.

The influence of suction on velocity profiles and velocity fluctuations was investigated as well.

The air expense through each slot was chosen on the basis of the single principle: it must be sufficient to provide laminar flow behind the streamwise next slot. Thus, the optimum value of Q_1 through the first slot was considered to be that at which the chordwise distribution of ε reached a minimum just behind the second slot. The air expense through the second slot was determined from similar considerations. The suction scheme described has allowed the extent of the boundary layer's laminar part to be increased from 40 to 70 percent of the chord.

4.2 Numerical simulation of laminar - turbulent transition with considering boundary layer suction

Calculations were performed using unstructured computational mesh (Figure 16), consisting of 51.3 million elements and 18.8 million nodes. In the boundary layer zone a special finite-difference mesh consisting of 50 layers of prismatic elements was created. The thickness of the first prismatic layer was 0.005 mm (relative height of the first cell of the computational grid $y^+ \leq 1$). Total number of prismatic elements is equal to 30 million.

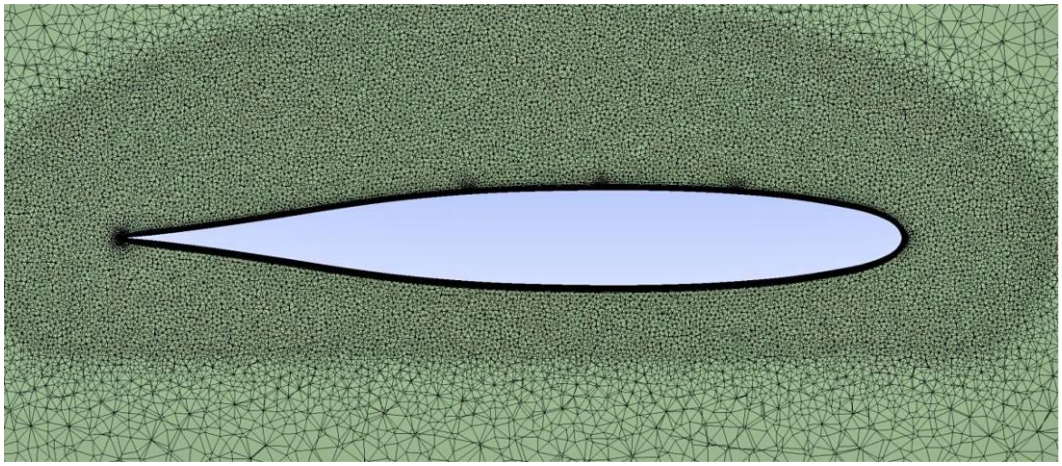

Figure 16: SR0012 wing CFD mesh

The following cases of flow over a wing were considered both in calculations and experiment:

- Case No.1 – flow without suction;
- Case No.2 – suction from the first slot at $\mathrm{Re}_{1,s} = 140$;
- Case No.3 – suction from the first slot at $\mathrm{Re}_{1,s} = 216$;
- Case No.4 – suction from the first slot at $\mathrm{Re}_{1,s} = 320$;
- Case t No.5 – suction from the first and second slots at $\mathrm{Re}_{1,s} = \mathrm{Re}_{2,s} = 216$;
- Case No.6 – suction from the through all three slots at $\mathrm{Re}_{1,s} = \mathrm{Re}_{2,s} = 216$; $\mathrm{Re}_{3,s} = 100$

Influence of boundary layer suction on the position of the laminar-turbulent transition was calculated using two models of turbulence – γ-Re_θ and γ- models. The calculated and experimental values of the coordinates of the transition beginning in the central section of the wing, depending on the case of the suction of the boundary layer, are shown in Figure 17.

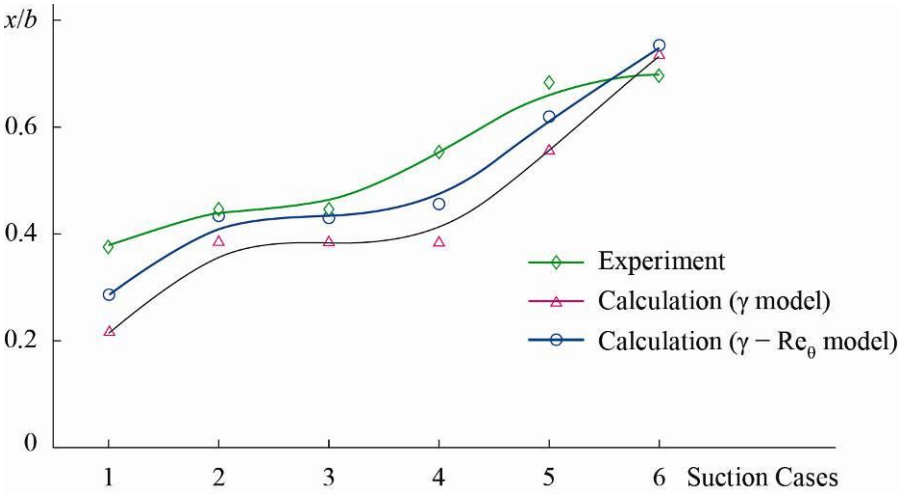

Figure 17: The position of transition in the central section of the wing, depending on the case of the suction

It can be noted that both models provide an acceptable agreement with the experiment. Langtry and Menter $\gamma - \mathrm{Re}_\theta$ model shows the results closer to the experimental ones. Compared with the results of measurements CFD-calculation predicts earlier transition. With both models calculations were performed using standard values of the model coefficients. Perhaps

the selection of model coefficients can adapt this model for better simulation of the experiment described above, but these studies have not been conducted in the framework of this study.

5 CONCLUSIONS

- The detailed experimental investigations of the transition zone on the straight and swept wings were carried out in the low-turbulence T-124 TsAGI wind tunnel. The influences of the incoming flow turbulence, acoustic disturbances and local boundary layer suction were studied. The validation of various transition prediction methods by comparison of experimental and calculated data obtained under the simulated influence of the above-mentioned factors was performed.
- The possibilities of application of different turbulence models for prediction of the laminar-turbulent transition and for investigation of the increased free stream disturbances and boundary layer suction effects on the transition characteristics in 2D and 3D flow are analyzed.
- The Walters-Cokljat and Langtry-Menter $\gamma - \mathrm{Re}_\theta$ turbulence models enable, in principle, to predict the laminar-turbulent transition in the cases when the cross-flow instability is insignificant. Compared with the transition model of Walters-Cokljat based on the transport equation for laminar and turbulent kinetic energy, $\gamma - \mathrm{Re}_\theta$ model is more versatile since it allows calculate the intermittency in the transition zone.
- The possibility of taking into account the cross-flow instability is realized in new Local-Correlation-Based Transition Model (γ - model). This model solves only one transport equation for the intermittency γ and allows the detection of cross-flow instability with the use of the Arnal C1-criterion.
- Both $\gamma - \mathrm{Re}_\theta$ and γ - model give acceptable results when modeling the influence of the increased level of free-stream turbulence and boundary-layer suction on the laminar-turbulent transition on the straight and swept wings. However, for application in specific conditions the fine tuning of the models is required. So additional researches are necessary to define the operational limits for each of the laminar-turbulence transition models to develop recommendations for their practical use.
- The empirical and semi-empirical models, allowing estimate the location of transition basing only on the averaged flow characteristics are still very robust and effective means for laminar-turbulent transition prediction at elevated free-stream turbulence level, at least in 2D boundary layers. Some of empirical criteria permit to calculate the location of transition on the swept wings, but they can't be applied at high level of free-stream turbulence.
- The e^N-method rather successfully correlates with laminar-turbulent transition for 2D boundary layer; however, the values of N-factor corresponding to transition are substantially different for various external conditions. Contrary to the 2D flows, for the swept wing boundary layer the semi-empirical e^N -method gives substantial scatter of the critical N-factor values and does not permit to correlate reliably the transition data. The reason of this phenomenon is dominating of the non-linear effects in the transition processes in the 3D boundary layer even at low level of the external turbulence.

REFERENCES

[1] S.L. Chernyshev, A.I. Ivanov, A.Ph. Kiselev, V.A. Kuzminsky, D.S. Sboev, S.V. Zhigulev, Investigations of influence of free stream turbulence and acoustic disturbances on the laminar-turbulent transition on LV6 airfoil and swept wing models. *AIAA Paper 2011-210*, 18 p., 2011.

[2] V.A. Vlasov, S.V. Zhigulev, A.I. Ivanov, A.Ph. Kiselev, V.A. Kuzminsky, D.S. Sboev, S.L. Chernyshev, Laminar-turbulent transition on the LV6 laminarized airfoil: natural transition. *TsAGI Science Journal*, **42**, No. 5, 565-591, 2011.

[3] V.A. Vlasov, S.V. Zhigulev, A.I. Ivanov, A.Ph. Kiselev, V.A. Kuzminsky, D.S. Sboev, S.L. Chernyshev, Laminar-turbulent transition on the LV6 laminarized airfoil. Part II: effect of free stream disturbances. *TsAGI Science Journal*, **42**, No. 6, 729-756, 2011.

[4] O.V. Babich, P.P. Vorotnikov, A.Ph. Kiselev, L.L. Chernyshev, S.L. Chernyshev, Laminar flow control on low-sweep wing. *Book abstracts of International Conference on Fundamental Research in Aerospace Science (1st FRAS)*, Section 1, 6–9, Zhukovsky, Russia, September 22-24, 1994.

[5] S.L. Chernyshev, A.I. Ivanov, A.Ph. Kiselev, V.A. Kuzminsky, D.S. Sboev, L.L. Teperin , V.V. Vozhdaev, Comparison of the laminar-turbulent transition prediction using different methods with the laminar wing test results. E. O˜nate, J. Oliver and A. Huerta eds. *Proceedings of 11th World Congress on Computational Mechanics (WCCM) / XI 5th European Conference on Computational Mechanics (ECCM V) / 6th European Conference on Computational Fluid Dynamics (ECFD VI)*, **5**, 6310-6321, Barcelona, Spain, July 20 -25, 2014.

[6] S.L. Chernyshev, A.I. Ivanov, A.Ph. Kiselev, V.A. Kuzminsky, D.S. Sboev, The free-stream turbulence effect on the laminar-turbulent transition in the swept wing boundary layer. E. O˜nate, J. Oliver and A. Huerta eds. *Proceedings of 11th World Congress on Computational Mechanics (WCCM XI) / 5th European Conference on Computational Mechanics (ECCM V) / 6th European Conference on Computational Fluid Dynamics (ECFD VI)*, **6**, 7511-7520, Barcelona, Spain, July 20 -25, 2014.

[7] R. Langtry, F.R. Menter, Correlation-based transition modeling for unstructured parallelized computational fluid dynamics codes, *AIAA Journal*, **47**, No. 12, 2894-2906, 2009.

[8] D.K. Walters, D. Cokljat, A three-equation eddy-viscosity model for Reynolds-averaged Navier-Stokes simulations of transitional flows, *Journal of Fluids Engineering*, **130**, No. 12, 121401–1 – 121401–14, 2008.

[9] F.R. Menter, P. Smirnov, Laminar-Turbulent Transition Modelling based on a New Intermittency Model Formulation. *11th World Congress on Computational Mechanics (WCCM XI) / 5th European Conference on Computational Mechanics (ECCM V) / 6th European Conference on Computational Fluid Dynamics (ECFD VI)*, Barcelona, Spain, July 20 -25, 2014.

[10] V.M. Filippov, Characteristics of fluctuations in flow through low-turdulence arerodynamic wind tunnel T-124 designed for small speeds. *Uchenye Zapiski TsAGI.* **39**, No.1-2, 68-80, 2008 (in Russian).

[11] R. Narasimha, The laminar-turbulent transition zone in the boundary layer. *Progress in Aerospace Sciences*, **22**, No. 1, 29-80, 1985.

[12] R.E. Mayle, The role of laminar-turbulent transition in gas turbine engines. *Journal of Turbomachinery*, **113**, No. 4, 509-537, 1991.

[13] D. Arnal, M. Habiballah, E. Coustols, Theorie de l'instabilite laminaire et criteres de transition en ecoulement bi et tridimensionnel. *La Recherche Aerospatiale*, No. 2, 125-143, 1984.

[14] A.Ph. Kiselev, V.A. Kuzminsky, D.S. Sboev, The laminar-turbulent transition zone in 2D and 3D boundary layers with emphasis on effect of free stream turbulence. *29th Congress of the International Council of the Aeronautical Sciences (ICAS 2014)*, St. Petersburg, Russia, 7-12 September, 10 p., 2014г.

[15] W.J. Solomon, G.J. Walker, J.P. Gostelow, Transition length prediction for flows with rapidly changing pressure gradients. *Journal of Turbomachinery*, **118**, No. 4, 744-751, 1996.

[16] S.K. Roberts, M.I. Yaras, Modeling transition in separated and attached boundary layers. *Journal of Turbomachinery*, **127**, No. 2, 402-411, 2005.

[17] W.B. Brown, A stability criterion for three-dimensional laminar boundary layers. in *Boundary layer and flow control.* **2**. Pergamon Press, 913-923, 1961.

[18] V.A. Barinov, V.M. Lutovinov, On the parameters of approximate relationship of critical Reynolds number in the three-dimensional boundary layer. *Uchenye Zapiski TsAGI*, **4**, No. 4, 27-32, 1973 (in Russian).

[19] M.V. Usinov, Statistical description of laminar-turbulent transition in a boundary layer at high freestream turbulence degree. *Fluid Dynamics*, **48**, No. 2, 192-200, 2013.

[20] V.A. Kuzminsky, Matrix numerical method of stability calculation of three-dimensional boundary layers. *Uchenye Zapiski TsAGI*. **38**, No. 3-4, 44-56, 2007 (*in Russian*).

[21] L.M. Mack, Transition prediction and linear stability theory. *AGARD CP*-224, 11-22, 1977.

[22] D. Arnal, Boundary layer transition: predictions based on linear theory. *Special course on progress in transition modelling*. AGARD Rep. No. 793, 2-1 - 2-63, 1994

[23] H. Bippes, Basic experiments on transition in three-dimensional boundary layers dominated by crossflow instability. *Progress of Aerospace Sciences*, **35**, No. 4, 363-412, 1999.